

ANALYSIS OF SEAGRASS ABOVEGROUND CARBON STOCK DYNAMICS IN PARI ISLAND, 2021-2023, USING SENTINEL-2

Jennifer WIJAYA¹, Pramaditya WICAKSONO^{2,*}, Muhammad KAMAL²

¹ Master Programme in Remote Sensing, Faculty of Geography, Universitas Gadjah Mada, Yogyakarta, 55281, Indonesia

² Department of Geographic Information Science, Faculty of Geography, Universitas Gadjah Mada, Yogyakarta, 55281, Indonesia

Abstract

Seagrasses are marine plants that efficiently store carbon. Understanding their role in climate change requires information on seagrass area and carbon content, which is currently lacking in Indonesia. The objectives of this study are to (1) develop a mapping model of seagrass aboveground carbon stock (AGC) dynamics based on percents of seagrass cover, (2) map AGC dynamics using multitemporal Sentinel-2 imagery and (3) analyze patterns and factors affecting AGC dynamics. This study used two regression models, random forest regression (RFR) and stepwise regression (SWR). The RFR regression model produced a more accurate and consistent AGC map with $R^2=0.21$ ($RSME=5.04gC/m^2$) for the Ea class and $R^2=0.24$ ($RSME=1.99gC/m^2$) for the ThCr class. Meanwhile, SWR produced an accurate AGC map for the EaTh class with $R^2=0.15$ ($RSME=2.90gC/m^2$). Both models were applied to Sentinel-2 images for 15 months, from April 2021 to December 2023. The highest AGC for the RFR model was shown in October 2021 with 0.104 tons of carbon and for the SWR model in December 2023 with 0.105 tons from a total seagrass cover area of 1.15km². Biophysical variables like rainfall can affect AGC dynamics. As rainfall increases, the AGC estimate tends to increase.

Keywords: Seagrass; Species composition; Percent cover; Aboveground carbon stock; Sentinel-2; mapping

Introduction

Climate change and global warming represent significant international challenges, given their profound impacts on human life and the environment. These phenomena can result in a number of adverse effects, including an increased frequency and intensity of extreme weather events, changes in sea surface temperatures, rising sea levels and alterations in seawater pH [1]. One strategy for addressing the impacts of climate change is the utilization of blue carbon ecosystems, which include mangroves, seagrasses and algae. The effective management and utilization of these ecosystems can assist in the mitigation of the impacts of climate change by supporting the ecosystem services of carbon sequestration, biodiversity preservation and coastal protection [2, 3].

Seagrass is a type of marine vegetation that has the capacity to absorb and store carbon in an effective and efficient manner [4]. As autotrophic plants, seagrasses bind carbon dioxide and convert it into energy, contributing to their high primary productivity. This energy enters the food chain either through direct predation by herbivores or through decomposition as litter [5]. Seagrass carbon stocks can be measured in both aboveground and belowground components. The

* Corresponding author: prama.wicaksono@mal.ugm.ac.id

term 'aboveground carbon stock' (AGC) refers to the carbon stored in seagrass parts above the sediment surface, including stems, leaves and flowers [6].

Seagrasses cover only approximately 2% of the ocean but can sequester up to 15% of the total oceanic carbon [7-9]. In Indonesia, seagrass meadows have the potential to cover 1.847.341 hectares [9], though only 293.464 hectares have been verified. These verified areas are estimated to sequester between 1.6 and 7.4 Tg C/year [9]. Approximately 12 species of seagrasses are distributed across Indonesia's coastal waters [5], each with varying carbon storage capacities due to differences in size. According to Kennedy and Björk [10], seagrass species with larger morphological forms tend to have greater biomass, thus exhibiting higher carbon accumulation capacities. Therefore, in order to understand the potential of each seagrass species in carbon storage, it is necessary to have knowledge of their distribution in specific areas. A comprehensive inventory of seagrass species, including their spatial distribution and carbon stock, is essential for optimizing the use of seagrass ecosystems. Such data can inform policies for environmental conservation and the sustainable use of marine resources [11-13]. However, data on the distribution and condition of seagrasses in Indonesia remain limited and require further validation [4, 5].

Access to seagrass habitats is challenging due to environmental influences and habitat complexity. Field survey methods for data acquisition are time-consuming, costly and lack spatial extensiveness, particularly over time [14-16]. A rapid assessment is necessary because the validated seagrass area in Indonesia is yet to reach the potential 1.8 million hectares of seagrass ecosystems [9]. One effective approach is to utilize remote sensing technology in conjunction with field measurement data to map percent cover (PC) and seagrass above-ground carbon stock (AGC) [17, 18]. This method provides a non-destructive alternative for obtaining seagrass AGC data by interpreting biophysical aspects of seagrass, such as percent cover, through remote sensing [19-24]. *A.J. Wahyudi et al.* [24] demonstrated that seagrass PC is strongly correlated with AGC, with a higher PC value indicating greater carbon storage potential. Consequently, rapid assessments of seagrass AGC based on PC data, in conjunction with existing formulas, can effectively estimate seagrass AGC.

Nevertheless, the applicability of existing seagrass AGC mapping models across diverse locations with varying environmental conditions and species distributions remains uncertain [25]. Furthermore, the efficacy of these methods in multi-temporal studies, considering seasonal or long-term environmental changes, is yet to be fully elucidated [26]. Additional challenges include the limitations of remote sensing in estimating seagrass AGC due to factors such as tidal influences, benthic habitat complexity and the spectral reflectance similarity of benthic habitats. Consequently, there is a need to develop a seagrass AGC mapping model that addresses these challenges.

The objective of this study is to develop a mapping model for seagrass AGC dynamics at the species composition level using non-destructive methods based on Sentinel-2 reflectance values and seagrass PC. The developed model will be used to map AGC dynamics using multitemporal Sentinel-2 images and to analyze patterns and factors influencing seagrass AGC dynamics in the study area. The choice of Sentinel-2 imagery was motivated by its free availability and extensive coverage of the Earth's surface, rendering it a promising tool for seagrass and benthic habitat mapping [27-30]. Furthermore, Sentinel-2 offers a spatial resolution suitable for local- to national-level mapping and a high temporal resolution of 5-10 days, which is beneficial for monitoring seagrass AGC dynamics and understanding seasonal and long-term changes in seagrass ecosystems [29].

The research was conducted on Pari Island, located in Kepulauan Seribu, within the administrative area of DKI Jakarta Province (Fig. 1). This site was selected due to its extensive seagrass coverage and species diversity [31].

However, the seagrass ecosystem on Pari Island has been degraded by human activities such as reclamation, coastal development, pollution and destructive fishing practices, as well as by climate change [31]. These factors have led to significant changes in seagrass cover on the island [32]. Variations in the percentage of seagrass cover affect the seagrass carbon stocks on

Pari Island. Therefore, it is crucial to map the dynamics of seagrass AGC to understand the spatial and temporal distribution and factors influencing these dynamics. The analysis results are essential for developing conservation policies aimed at reducing exploitation, preventing damage and preserving the ecological role of seagrass beds in coastal ecosystems.

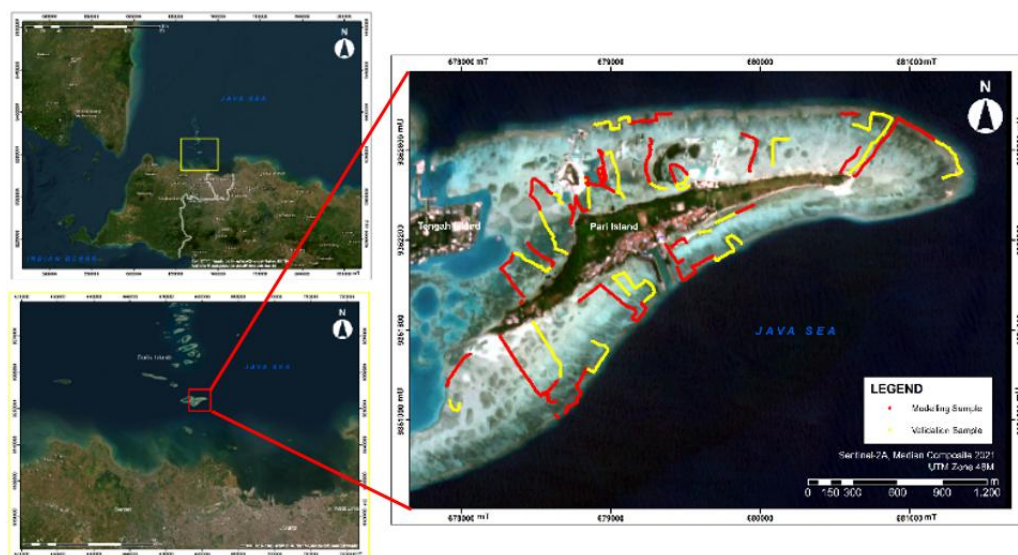


Fig. 1. The distribution of photo-transect samples collected during a field survey that took place from February 27 to March 3, 2023. These samples are overlaid on a Sentinel-2A image median composite of April 2021

Experimental part

Materials

The Sentinel-2 image utilized in this study was obtained at Level 2A (L2A), which has undergone atmospheric correction to yield surface reflectance (SR) data. This study exclusively utilized bands with a spatial resolution of 10 meters, specifically blue (B2 - centered at 492.4 nm), green (B3 - 559.8nm), red (B4 - 664.6nm) and near-infrared (B8 - 832.8nm). The imagery has a radiometric resolution of 12 bits and is projected using the Universal Transverse Mercator (UTM) system within the 48 M zone. Sentinel-2A images from April 2021 to December 2023 were analyzed at intervals of two to three months (Table 1). Monthly median composites were obtained from multitemporal images of the selected months to enhance image quality and mitigate disturbances such as cloud cover or noise [33]. Median composites are particularly resilient to abrupt changes caused by disturbances in individual temporal images, as the median value is more stable compared to the mean or maximum value [34].

Table 1. Sentinel-2A images used in this research

Year	Month	Dates	Year	Month	Dates
2021	April	9, 14, 24, 29	2023	January	9, 14, 24
	June	8, 13		April	9, 14, 19, 24, 29
	August	7, 12, 17, 27		June	3, 28
	October	6, 11, 16, 26		August	7, 12, 17, 22, 27
2022	January	4, 24	October	11, 16, 21, 26, 31	
	March	5, 10, 20	December	10, 15, 20, 25, 30	
	May	14, 24, 29			
	August	7, 12, 17			
	November	5, 25			

The selected image conditions for analysis were cloud-free, low tide and sunglint-free. Consequently, no water column or sunglint correction process was necessary. Fifteen monthly median composite Sentinel-2A images, spanning three years, were used to map seagrass AGC. However, the median composite images for the months of February and March 2023, which coincided with the field data collection, exhibited a high level of cloud cover, rendering them unsuitable for the construction of seagrass AGC mapping models. Consequently, the image used for the construction of the remote sensing model for AGC mapping was the median composite image from April 2023, as it was the closest alternative.

Methods

Field Survey

The field survey was conducted between 27 February and 3 March 2023. The transect lines were established based on the visual similarity of the spatial distribution of benthic habitat cover observed in the images (Fig. 1). Samples in the form of benthic photos were collected using the photo-transect method [35] along the transect line by snorkeling with an underwater camera, maintaining an interval of approximately 1 meter between photos. A GPS device in tracking mode recorded coordinates every 2 seconds, synchronized with the camera's clock.

The benthic photos were geotagged and analyzed using CPCe software to measure benthic habitat cover and identify seagrass species in each photo. Seagrass PC data were utilized to calculate the AGC values based on the PC-AGC equation [17]. The dataset was partitioned into 70% for model creation and 30% for validation. The selection of model and validation samples was conducted by considering the spatial distribution of samples, species variations and variations in seagrass PC. In total, 1711 photos of benthic habitat were collected, with 1172 designated for mapping model development and 539 for validation. Of these, 710 samples were classified as seagrass and used for seagrass species composition mapping and AGC mapping model development. The seagrass samples were subsequently classified into three categories: 189 samples of the Ea class, 550 samples of the ThCr class and 46 samples of the EaTh class. For a detailed description of each seagrass species composition class, please refer to Table 2.

Benthic Habitat Classification and Seagrass Species Composition Mapping

Benthic habitat mapping was conducted with the objective of obtaining mask data for seagrass species mapping and in the empirical modeling of seagrass AGC at the species level. The classification scheme for benthic habitat mapping includes three primary categories: coral, seagrass and bare substrate. Given the non-clustered distribution of benthic habitats in the waters around Pari Island, the scheme was adjusted to include combination and mixed classes. For the purpose of seagrass species and AGC mapping, only pixels classified as the dominant seagrass class and the combination or mixed seagrass class were utilized.

Mapping the distribution of seagrass species is essential for obtaining species boundaries in seagrass AGC mapping, as each species has a different capacity for storing AGC. However, this mapping process is challenging due to the similar reflectance values of different seagrass species, even when using hyperspectral data [36]. Consequently, a refined classification scheme for seagrass species was developed, based on attributes such as life form variation [14]. Details of each seagrass species composition class are provided in Table 2.

Table 2. Classification scheme of seagrass species composition used for mapping based on Wicaksono and Hafizt [14]

Species Composition Class	Class Description
Ea	Area dominated by Ea ($\geq 80\%$)
EaTh	Mixed area of Ea, Th and Cr with relatively proportional composition. Cs, Si and Ho can also be found with minor percentage
ThCr	Mixed area between Th and Cr with relatively proportional composition. Cs, Si and Ho can also be found with minor percentage

The classification of benthic habitat and seagrass species composition was conducted using the random forest (RF) algorithm. The RF algorithm operates by constructing multiple decision trees and combining their outputs to achieve more stable and accurate predictions [37]. This study evaluated four scenarios with varying numbers of trees: 50, 100, 200 and 300. The RF algorithm requires functions for random feature selection and impurity assessment during its operation [38–40]. In this study, all used combinations of functions on randomly selected features in the form of square root and log and impurity functions in the form of gini and entropy. The selection of benthic habitat classification results and seagrass species composition for empirical AGC modeling was based on the stability and consistency of the RF algorithm's accuracy. This accuracy was measured in terms of overall accuracy (OA), producer's accuracy (PA) and user's accuracy (UA) from the confusion matrix for each model's accuracy assessment.

AGC Mapping

The AGC of each seagrass species was derived from seagrass PC data collected from field surveys using the PC-AGC equation at the species level, developed by *P. Wicaksono et al.* [17]. The seagrass PC data for each species was used to calculate the AGC based on species composition classification. The specific PC-AGC formulas employed are detailed in Table 3.

Table 3. Equations to convert seagrass PC to AGC used in this research [17]

Seagrass Species	PC-AGC Equation
<i>Enhalus acorodies</i> (Ea)	$AGC_{Ea} = 0.3179(PC_{VEa}) + 0.6295$
<i>Thalassia Hemprichii</i> (Th)	$AGC_{Th} = 0.1069(PC_{VTh}) + 0.0951$
<i>Cymodocea rotundata</i> , <i>Halodule univervis</i> (CrHu)	$AGC_{CrHu} = 0.0604(PC_{VCrHu}) - 0.1767$
<i>Syngodium isoetifolium</i> , <i>Halophila ovalis</i> (SiHo)	$AGC_{SiHo} = 0.00268(PC_{VSiHo}) - 0.0022$
<i>Cymodocea serrulata</i> (Cs)	$AGC = 0.1028(PC_r) + 1.449$ (community-level equations)

In the study area around Pari Island, the species *Cymodocea serrulata* (Cs) was identified. However, this species lacks a specific PC-AGC equation in the referenced literature, necessitating the use of a community-level equation for AGC calculations. The samples were then divided into two sets: one for training the regression model and another for assessing the accuracy of the resulting AGC map.

The seagrass AGC mapping model was developed using Sentinel-2A monthly median composite data, employing two regression techniques: random forest regression (RFR) and stepwise regression (SWR). RFR minimizes the error between predicted and reference values through a non-parametric algorithm that iteratively generates a regression model [41, 42]. During the model development process, a number of Random Forest Regression (RFR) parameters were tested, including the number of trees (n_{Tree} : 50, 100, 200, 300), functions (square root and user-specified number of features or m_{try}) and the minimum number of samples in nodes (2, 3, 5 and 10). The optimal RFR parameter combination was then applied to multitemporal images to analyze AGC dynamics using the RFR mapping model. SWR is an automated procedure that selects the most predictive variables for the regression model [43, 44]. The SWR process identifies the optimal predictors to include, utilizing solely the bands selected in the final stepwise model for monthly multitemporal imagery analysis.

The accuracy of seagrass AGC mapping was evaluated using the correlation coefficient (r) and the coefficient of determination (R^2) and root mean square error (RMSE) values based on independent field data. The most accurate regression models from RFR and SWR were employed in this study to ascertain the most suitable model for each monthly multitemporal image.

Multitemporal Analysis

A multitemporal seagrass AGC map was obtained and the AGC of seagrasses over 15 months was calculated. Monthly changes in AGC were then assessed. To analyze the factors

influencing seagrass AGC dynamics, AGC values were compared with various environmental parameters. The factors affecting the dynamics of seagrass AGC include changes in chlorophyll-a concentration, rainfall, salinity and sea surface temperature (SST) [44]. Monthly average rainfall data were sourced from the Climate Hazards Group InfraRed Precipitation with Station (CHIRPS) [45], while data on chlorophyll-a concentration, monthly average salinity and monthly SST were obtained from Marine Copernicus [46]. Pearson correlation analysis was employed to measure the statistical relationships between monthly variations in seagrass AGC and the environmental factors of chlorophyll-a concentration, salinity, rainfall and SST. Furthermore, the multitemporal seagrass AGC results were employed to ascertain the consistency of AGC at each pixel by utilizing the coefficient of variation technique.

Flowchart

The flowchart of this research is shown in Fig. 2.

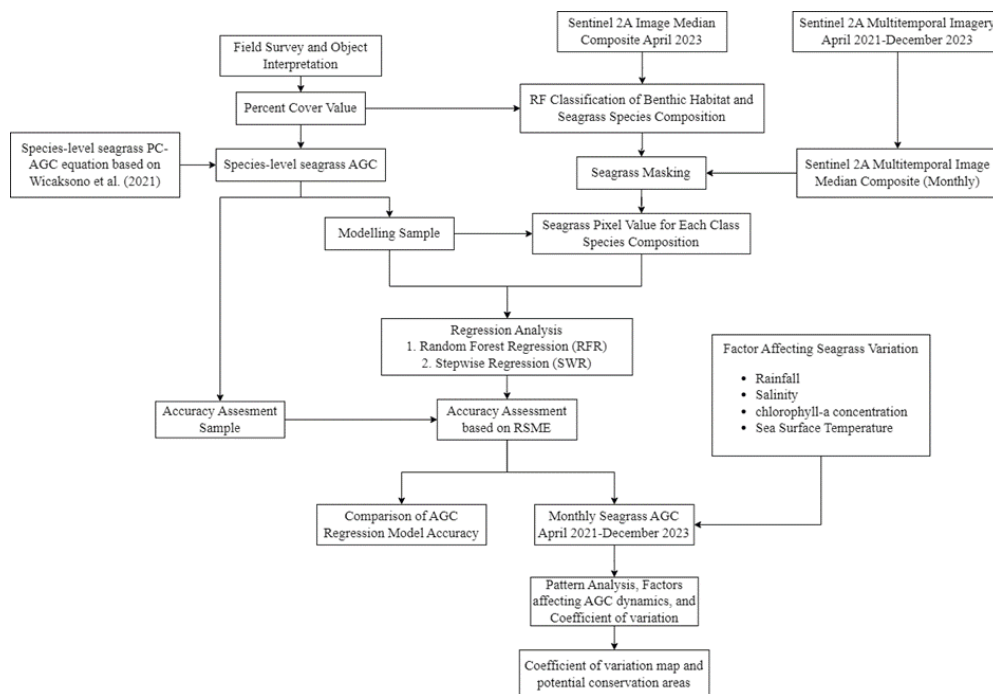


Fig. 2. Research flowchart

Results and discussion

Benthic Habitat Mapping

Figure 3 illustrates the benthic habitat map achieved using the RF algorithm with the highest accuracy (OA 51.02%). The experimental results from various hyperparameter scenarios indicate that the optimal OA was obtained with the following hyperparameters: impurity function set to gini, randomly selected features set to the square root of the number of features and n_{Tree} set to 50. The classification identified nine benthic habitat classes, including three dominant classes and six combination or mixture classes (Table 4).

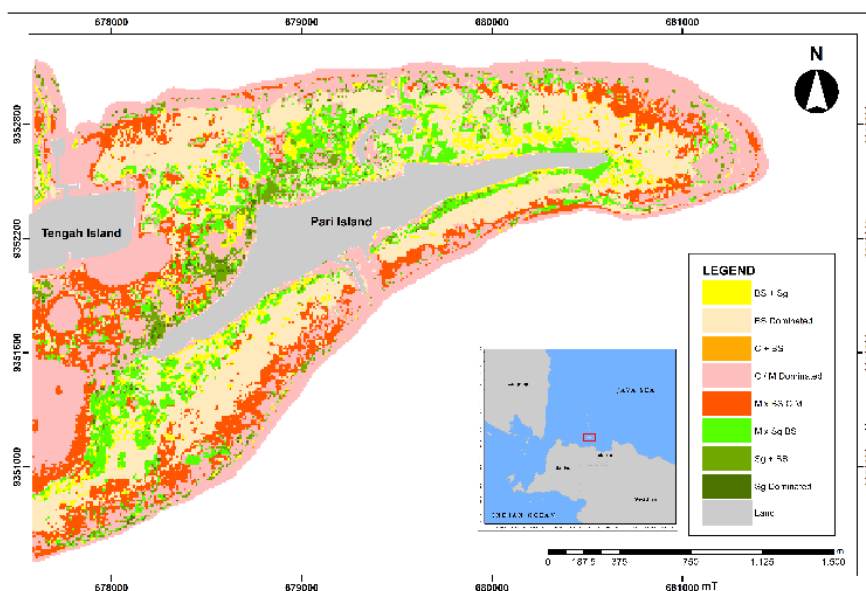


Fig. 3. Benthic habitat map obtained from RF classification algorithm with 51.02% OA

Table 4. Summary of UA and PA of the benthic habitat map with the highest OA

Benthic Class	Area (ha)	UA (%)	PA (%)	OA (%)
BS + Sg	33.05	22.92	18.03	51.02
BS Dominated	120.50	48.18	67.35	
C + BS	0.54	33.33	20.00	
C + M Dominated	156.77	72.30	26.43	
Mix BS C M	66.16	63.49	53.33	
Mix Sg BS	59.03	38.67	34.12	
Sg + BS	21.28	31.58	31.58	
Sg Dominated	2.06	37.50	16.67	

The classification of these classes was determined solely by the dominant class and detailed classes in the form of combination classes and mixed classes of the four benthic habitat types of bare substrate (BS), seagrass (Sg), coral (C) and macroalgae (M). The dominant class is a class with a PC value of a benthic habitat $\geq 80\%$ or when the PC of other undescribed habitats $\leq 20\%$. In this study, the dominant class is divided into three classes, namely the dominant class of seagrass (Sg Dominated), the dominant class of open substrate (BS Dominated) and the dominant class of macroalgae and coral (C + M Dominated). Coral and macroalgae classes are combined because most macroalgae in the study area are associated with coral reefs, so it is difficult to distinguish them. Besides that, the PC of macroalgae that stands alone is too small, causing the classification results to be less significant. The combination class is formed if there is a PC difference between classes of $> 20\%$ and each class has a PC of $> 20\%$. This class is characterized by the addition (+) in the class name, such as the combination class of bare substrate and seagrass (BS + Sg). Meanwhile, a mixed class is formed if the classes have a PC difference of 20%. One example of this class is a mixed class between bare substrate, coral and macroalgae (Mix BS C M).

One factor contributing to the suboptimal RF classification results is the influence of the background object in a pixel, specifically bare substrates (BS). For example, BS such as mud appear darker in images and may be misclassified as seagrass, while dead and destroyed coral

reefs may be misclassified as BS. The seagrass-dominated (Sg Dominated) class is underestimated, as the UA is 37.5% and the PA is 16.67%. This underestimation is due to the misclassification of seagrass as BS or a mixed seagrass class. Conversely, the BS Dominated class is overestimated, with a PA of 67.35% and a UA of 48.18%. The UA and PA values for the benthic habitat classification are detailed in Table 4.

Although the classification results are moderately accurate, the derived benthic habitat distribution aligns well with actual field conditions, as evidenced by field survey results. The study area encompasses a total benthic habitat area of approximately 4.59km², predominantly consisting of BS Dominated (120.5ha) and C+M Dominated (156.77ha) classes. In contrast, the area dominated by seagrass occupies a much smaller area, approximately 2.06ha. The majority of seagrass in the study area is mixed with BS (115.42ha).

Seagrass Species Composition Mapping

The seagrass species composition map with the highest OA is 62.19%, achieved using the hyperparameters impurity = entropy, randomly selected features = square root and $n_{Tree} = 200$. This accuracy is lower than that observed in previous studies. For example, research by *P. Wicaksono and W. Lazuardi* [47] obtained a seagrass mapping OA of 70.37% using WorldView-2 imagery, while Ariasari et al. [48] achieved an OA of 83.52-85.71% for seagrass species composition mapping using PlanetScope imagery and RF classification.

Table 5 indicates that the ThCr and Ea classes are the most accurate, as indicated by their high UA and PA. This is likely because these classifications consist of a single life form with similar leaf morphology. In contrast, the EaTh classification appears significantly underestimated, with a UA of 25% compared to a PA of 5.88%. This discrepancy suggests that most EaTh samples are misclassified as either Ea or ThCr. A number of factors contribute to this discrepancy, including the relatively small sample size for the EaTh class.

Table 5. Confusion matrix of seagrass species composition classification using RF. The highlighted columns indicate the number of reference data correctly classified

Class	Reference			Total	UA (%)
	Ea	EaTh	ThCr		
Ea	30	8	7	45	63.83
EaTh	0	1	2	3	25.00
ThCr	11	7	84	102	64.62
Total	41	16	93	150	
PA (%)	68.83	5.88	66.14	OA (%)	62.19

The misclassification of seagrass species composition mapping can be attributed to the similar reflectance values of seagrass species, particularly in the ThCr and EaTh classes, which complicates their distinction using random forest classification. In addition, the influence of background objects also accompanies the reflectance recorded by the sensor, which in this case is a bare substrate [49]. It is also possible that the shallow marine habitat maps produced previously were also affected by background objects in the form of open substrates that are more dominant and affect seagrass objects so that the percentage of seagrass cover for seagrass species composition mapping has been reduced.

The seagrass cover area on Pari Island is approximately 115.42 ha, with the following composition classes: Ea (23.65ha), EaTh (5.89ha) and ThCr (85.88ha) (Fig. 4).

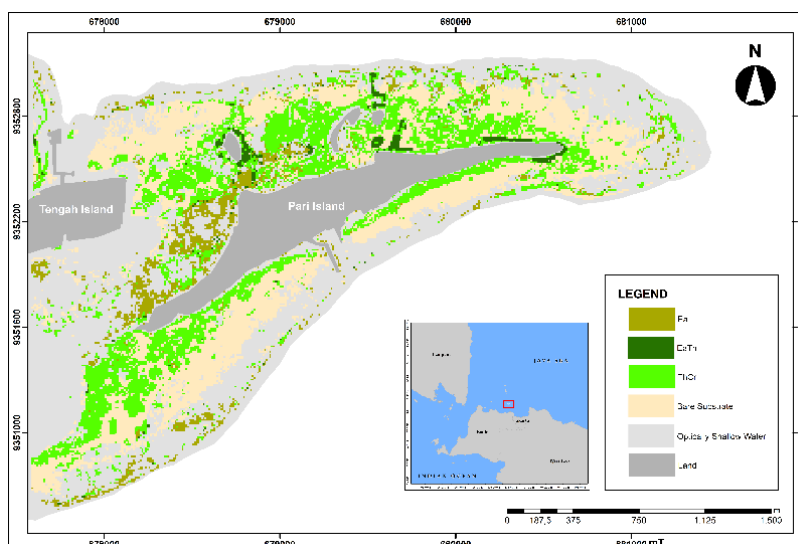


Fig. 4. Seagrass species composition map obtained from RF classification algorithm with OA 62.19%

The distribution of seagrasses tends to be clustered in the northern part of the island, where Ea, Th and Cr species dominate and are heterogeneously distributed along the coast. The ThCr composition class is the most prevalent in the study area. The Ea species composition class is primarily found along the northern coast and the southern part towards the optical deep sea. The EaTh composition class, which includes all types of seagrass species, is mainly located in the northern region of the study area. These mapping results of seagrass species composition were utilized to create masks for each composition class, serving as boundaries for species-level AGC modeling.

Seagrass AGC Mapping Model Development

Table 6 presents the range of seagrass AGC, calculated based on the PC of each seagrass species in each field data. In this study, the species-level AGC was utilized, as each seagrass species has different capacities for carbon storage, influenced by differences in canopy cover and rhizome structure, which affect the potential for carbon sequestration [50].

Table 6. Seagrass PC and AGC calculation results

Seagrass Species	PC			AGC (gC/m ²)		
	min	max	mean	min	max	mean
Ea	0.83	96.00	13.32	0.95	31.15	4.47
Cs	1.00	4.00	0.03	1.55	1.76	1.58
Th	0.83	92.00	16.13	0.20	9.93	3.00
CrHu	0.83	81.00	7.36	0.005	4.72	0.34
SiHo	0.83	11.00	0.10	0.0005	0.02	0.0001
All species	0.83	99.00	37.06	1.09	31.15	9.44

The AGC values of seagrasses, determined using species-specific equations, range from 1092 to 31,148gC/m². Species Ea, a large species capable of growing to the water surface, has the highest average AGC due to its substantial size compared to species in other classes. *Thalassia hemprichii* (Th) typically grows in groups, either as a single species or mixed with others. Cr and Hu (CrHu) were analyzed together due to their similar morphology and life forms, with the primary visible difference being the shape of their leaf tips [41]. Although Si and Ho have different leaf shapes, their AGC values are almost identical, leading to combined AGC

calculations. Additionally, Si and Ho are smaller in size and occupy a limited area in the study site. Each seagrass species will be grouped by life form to form a species composition class. Ea species composition class consists of only one species, Ea, as the basis of AGC mapping. The ThCr species composition class consists of all seagrass species except Ea, while the EaTh composition class is a combined class of all seagrass species as the basis of its mapping.

The RFR and SWR regression models for species-level seagrass AGC mapping were applied to the median composite Sentinel-2A image of April 2023. The model was applied separately for each seagrass species composition class. The best regression model was evaluated using RMSE. Table 7 indicates that the AGC regression model using the RFR model has the lowest RMSE in the Ea and ThCr species composition classes. Conversely, the SWR yields the EaTh AGC mapping model with the lowest RMSE. However, the difference in the RMSE values between the two regression models for each species composition class is minimal. For the Ea species composition class, the AGC RMSE values with the RFR and SWR models are 5.04gC/m² and 5.37gC/m², respectively. For the EaTh species composition class, the AGC RMSE values with the RFR and SWR models are 2.90gC/m² and 2.55gC/m², respectively. For the ThCr class, the AGC RMSE values with the RFR and SWR models are 1.99gC/m² and 2.0gC/m², respectively.

Table 7. Accuracy assessment results of the seagrass AGC mapping

Class	Model			Accuracy Assessment Result		
	Model	R ²	Hyperparameter and Variable Importance for RFF /Regression function for SWR	r	R ²	RSME (gC/m ²)
Ea	RFR	0.15	Variable importance = All bands; green is a bit higher than red; red is a bit higher than blue; NIR is the lowest <i>n</i> _{Tree} = 50 <i>m</i> _{try} = Square root all features Minimum number of sample in node = 5	0.49	0.21	5.04
	SWR	0.18	$AGC_{Ea} = 25.937 + (-64.944 \text{ Green})$	0.39	0.16	5.37
EaTh	RFR	0.30	Variable importance = All bands; green is a bit higher than blue; blue is a bit higher than red; NIR is the lowest <i>n</i> _{Tree} = 300 <i>m</i> _{try} = Square root all features Minimum number of sample in node = 10	0.37	0.15	2.90
	SWR	0.23	$AGC_{EaTh} = 23.662 + (-69.433 \text{ Green})$	0.34	0.17	2.55
ThCr	RFR	0.30	Variable importance = All bands; red is a bit higher than green; green is a bit higher than blue; NIR is the lowest <i>n</i> _{Tree} = 50 <i>m</i> _{try} = 3 (by user) Minimum number of sample in node = 10	0.5	0.24	1.99
	SWR	0.22	$AGC_{ThCr} = 10.233 + (-61.053\text{Green}) + (42.880\text{Blue})$	0.45	0.19	2.06

Previous research by *P. Wicaksono et al.* [51] demonstrated that the RFR model, when applied to WorldView-2 images of Kemujan Island and Labuan Bajo, achieved higher and more consistent accuracy than the SWR model. Contrastingly, another study by *P. Wicaksono et al.* [52] found that the SWR model outperformed the RFR model in mapping seagrass AGC in Labuan Bajo using Sentinel-2 imagery. These findings indicate that the suitability of regression analysis models can vary based on the type of imagery, sample characteristics, seagrass distribution and variation and research location [25]. Additionally, temporal factors must be considered when applying a regression model to multitemporal images. Environmental dynamics, such as seasonal or long-term changes, can alter the patterns of seagrass AGC. Seagrass AGC is influenced not only by the ecosystem itself but also by temporal environmental conditions, indicating that the accuracy of regression models can be time-specific.

The RFR model for each species composition class produced higher *r* and *R*² values compared to the SWR model, with the exception of the *R*² value of the EaTh class. Nevertheless,

the discrepancies in r and R^2 values between the RFR and SWR models for each species composition class were not significant, indicating that the performance of the RFR and SWR models is relatively comparable. The low accuracy of SWR compared to RFR due to the use of linear regression is not suitable for AGC modeling using remote sensing. This is because factors such as biomass that influence AGC do not always show a linear relationship to remotely sensed vegetation structure. The RFR model results indicate that each seagrass species composition class requires different hyperparameter settings or combinations to achieve the optimal accuracy for the AGC regression model. *J. Rui et al.* [53] noted that there is no theoretical basis for determining the optimal hyperparameter values. The variation in hyperparameter settings leads to different accuracy values in each study, necessitating experimentation to identify the model that achieves the highest accuracy.

The two regression models demonstrate comparable optimal bands for seagrass AGC across different species compositions. In the Ea and EaTh classes, the green band performed the best in modeling AGC using both RFR and SWR techniques. This finding is consistent with previous studies that have highlighted the green band's significant role in AGC modeling across various image types and regression methods [41]. This influence is largely attributed to seagrass AGC being affected by leaf area index and chlorophyll, as seagrasses exhibit sensitivity to wavelengths between 500-600nm, encompassing the green band [36, 54]. Conversely, the ThCr class is more influenced by the red band. *Wicaksono et al.* [36] observed that species such as Cr, Ho, Si and Th exhibited high spectral reflectance values at wavelengths between 755-884nm, with Ea species also demonstrating high reflectance. In general, the NIR band is also considered an important variable for mapping AGC, which is also shown from the important variables where NIR also contributes to each seagrass species composition class. The waters in the median composite Sentinel-2A image of April 2023 are receding, especially on the southern coast of Pari Island. Small seagrass species dominate the area, so they are still below the water surface even though it is receding. This results in better performance of the Red band in AGC ThCr than the NIR band due to the weakening of the water column. Meanwhile, the northern part of Pari Island, dominated by Ea species, has deeper water conditions because it is close to the lagoon and turbid water conditions result in lower NIR band performance.

The variation in optimal bands for modeling the AGC of each species composition indicates that each species has a distinct spectral response sensitivity at specific wavelengths. For instance, species Ea exhibits a higher spectral response value than other species due to its denser PC and larger size [41]. However, AGC estimation errors for Ea species are common, often caused by the visual appearance of Ea cover in the image. In the images analyzed, the water conditions around the Ea species cover area were quite deep, so Ea was submerged in water and only the tips of the leaves were visible in the image's visual display. This condition led to an underestimation of the Ea AGC despite the species' high PC. In addition, because the data range of the Ea species composition class is wider, the accuracy of the AGC model for the Ea species composition class is smaller than the other classes. Additionally, the differing spectral responses of each species are influenced by their leaf area index (LAI), which is related to seagrass photosynthetic ability, chlorophyll content, shoot number and biomass [8, 54].

Based on the 1:1 plot (Fig. 5), the distribution of data on modeled and reference seagrass AGC for RFR and SWR shows similarities across different seagrass species composition classes. The ThCr class exhibits a more clustered data distribution compared to the Ea and EaTh classes. Both regression models tend to underestimate AGC values at higher ranges. A significant limitation of remote sensing for AGC modeling is the saturation effect of an object's spectral response at specific densities. Saturation occurs when the signal intensity of the object is either too high for the sensor to detect slight differences in intensity [55] or too low. When seagrass AGC values reach high levels, the model may become unresponsive to further changes in AGC

due to increased energy absorption in dense seagrass patches. This modeling limitation causes the predicted AGC values to no longer reflect variations accurately. The EaTh species composition class that grows spaced and mixed with other species or substrates can affect the pixel value of the image, resulting in saturation. In the Ea species composition class itself, saturation can occur, one of which is due to the high biomass value and because the substrate in the area is not clean carbonate sand, but there are microbenthos that also absorb energy. In addition, epiphytes on the leaves and turbid water conditions can also cause saturation. High AGC values tend to saturate due to the strong absorption of energy by seagrasses [17], compounded by the absorption of energy by the water column.

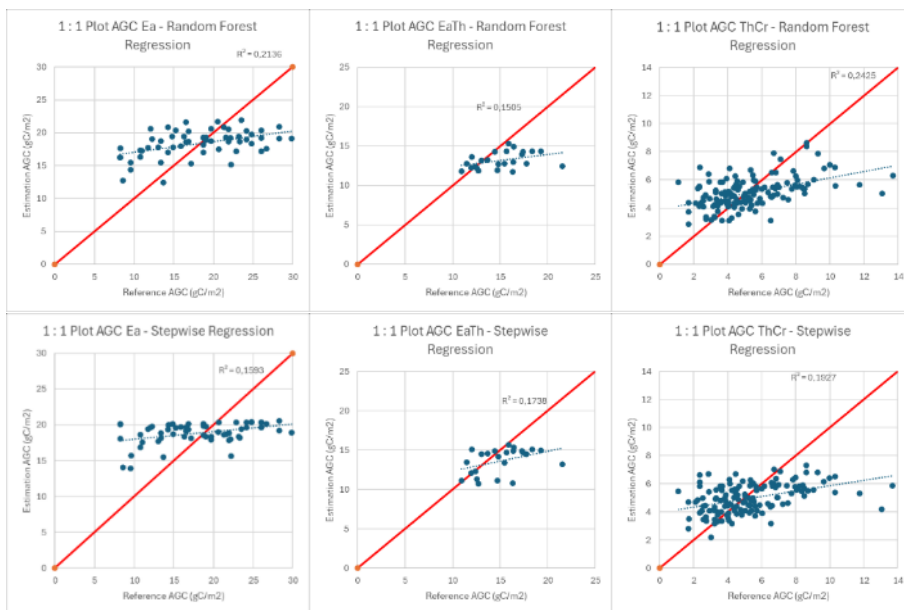


Fig. 5. The 1:1 plot between estimated and reference AGC for each species composition based on RFR and SWR

In addition to saturation, seagrass background has an effect in the form of an open substrate that can affect seagrass reflectance values [17]. Image pixel values as modeling variables have spectral responses susceptible to seagrass and environmental conditions. This can affect the strength and weakness of energy absorption in the spectral response [56]. The low accuracy of the resulting AGC modeling can also occur due to the lack of sample size, especially for the EaTh species composition class, because it has a small PC distribution. The accuracy results also show that species variations affect the spectral response of images for AGC modeling. Differences in each species' size, number of leaves and leaf structure can affect variations in AGC values and seagrass reflectance values in remote sensing images [57].

Seagrass AGC Mapping Model Application

The application of the RFR and SWR regression models produced a map of AGC in seagrass habitats, categorized by species composition classes, as illustrated in figures 6 and 7.

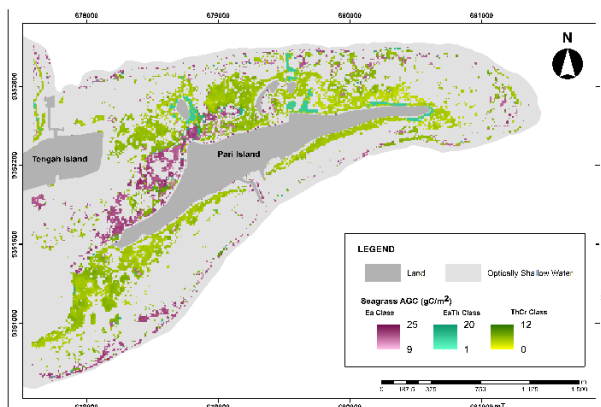


Fig. 6. Seagrass AGC map by species composition class in April 2023 using RFR with RMSE Ea 5.04; EaTh 2.90; ThCr 1.99

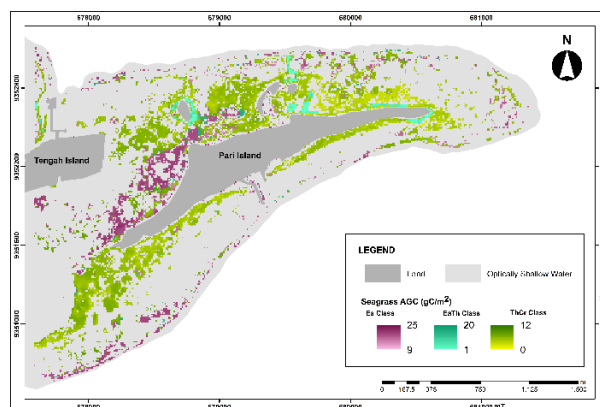


Fig. 7. Seagrass AGC map by species composition class in April 2023 using SWR with RMSE Ea 5.37; EaTh 2.55; ThCr 2.06

The estimated AGC values for the Ea class range from 9.31 to 23.54gC/m², for the EaTh class from 9.43 to 18.07gC/m² and for the ThCr class from 2.66 to 10.55gC/m². This translates to total AGC estimates of 0.043 tons C for Ea, 0.007 tons C for EaTh and 0.044 tons C for ThCR. Conversely, the SWR mapping model indicates AGC values of 9.36 to 21.70gC/m² for the Ea class, 3.44 to 17.11gC/m² for the EaTh class and 0.86 to 8.80gC/m² for the ThCr class. Consequently, the total AGC estimates derived from the SWR model are 0.043 tons C for Ea, 0.003 tons C for EaTh and 0.045 tons C for ThCr, which collectively cover a seagrass area of 115.42ha.

Based on the variation of AGC values in overall seagrass cover, the RFR model has slightly more variation in value than SWR. The difference between the estimated AGC value and the total estimated AGC of Ea and ThCr classes is not so large. However, quite different AGC estimates are shown in the EaTh class because of the lack of sample size for the EaTh class. SWR tends to be prone to overfitting and is very sensitive to variable selection and the order in which variables are included or removed from the model. The need for the required number of samples causes the SWR model to randomly select variables that match the modeled data without considering the match in the validation data. In addition, the EaTh class, a combination of all species in the study area, also affects the reflectance value of remote sensing image pixels, so the sensitivity of each regression model will be different.

The AGC maps generated from the two regression models show quite similar visuals because the difference in AGC estimates between the two is not so large. In the Ea and EaTh

species composition classes, the difference between the two is less visible, with the distribution of AGC estimates being quite similar. Meanwhile, the difference in AGC estimates for the ThCr species composition class can be clearly marked by differences in color gradation. The AGC map based on RFR appears to have darker color gradations or higher AGC estimates than the AGC map based on SWR. While gradation levels differ, both models depict similar distributions of high AGC values primarily along the northwestern coast. ThCr seagrass is concentrated in the southwest, while Ea is more prevalent in the north, despite ThCr having a wider distribution. Size differences among species contribute to the variability in AGC estimates. For instance, Ea may have a higher AGC value than ThCr despite its lower coverage. The northeastern coast generally shows lower AGC estimates due to sparse and less dense seagrass compared to the western part. As seagrass density declines towards the deep sea, AGC values also decrease, influenced by growth patterns and tidal dynamics.

Multitemporal Analysis of Seagrass AGC

This study employed RFR and SWR mapping models with optimal hyperparameter settings to map and analyze the dynamics of seagrass AGC from April 2021 to December 2023, covering a period of 15 months with intervals of two to three months. Figures 8-10 illustrate the dynamics of changes in mean and total AGC by species composition for both regression models.



Fig. 8. Average and total seagrass AGC of species composition class Ea



Fig. 9. Average and total seagrass AGC of species composition class EaTh

Based on the graph, there is an anomaly in the average dynamic pattern of AGC. The dynamics of AGC changes in the tropics typically reach a peak at the transition from the rainy season to the dry season [58]. Pari Island, part of the Thousand Islands archipelago located north of Jakarta, exhibits rainfall patterns similar to those observed in the capital city. The rainy season in the Thousand Islands spans from November to April, with peak rainfall occurring in January. From June to September, the region experiences the dry season, with the driest months usually

being July and August [59-60]. Given this information, an anomaly is observed in the average seagrass AGC pattern for January.



Fig. 10. Average and total seagrass AGC of species composition class ThCr

It is generally accepted that high rainfall has a negative impact on seagrass biomass. This is due to a number of interrelated factors, including increased sedimentation, decreased salinity, reduced light availability and physical damage to seagrass ecosystems [61]. It has been demonstrated that elevated rainfall enhances the flow of fresh water to the sea, which carries sediments that block sunlight, thus impeding seagrass growth. Additionally, decreased salinity and increased water turbidity further hinder seagrass by reducing water clarity and light penetration. Furthermore, high rainfall frequently results in increased cloud cover and algal blooms caused by eutrophication, both of which reduce light availability [62]. The intense water flow associated with heavy rainfall can also physically disrupt seagrass by uprooting or damaging the plants. The dynamics of AGC in seagrass exhibit a reasonably consistent pattern for Ea class. The RFR model indicates a decline in AGC in January 2021 and January 2023, with a peak in November.

One significant factor contributing to the abnormal multitemporal AGC dynamics pattern is the variability in the quality of the images used. The 15 images employed in the analysis exhibit differing qualities, which influence the reflectance values essential for mapping. These variations are likely due to the presence of fog, clouds and sunglint, which leads to poor radiometric quality. This indicates that a median composite image does not consistently provide the best quality. Despite the use of median compositing, the quality of the resultant monthly image still fluctuates based on the condition of the individual images. To mitigate this issue, the single-date image with the lowest initial cover for that month should be utilized. Consequently, seagrass AGC data for January was excluded from this analysis due to limited availability of remote sensing imagery.

The multitemporal seagrass AGC analysis revealed that the highest average total AGC peak for the RFR model occurred in October 2021, with a total carbon of 0.104 tons and for the SWR model in December 2023, with a total carbon of 0.105 tons. Conversely, the lowest average total AGC was recorded in November 2022 for the RFR model, with a total of 0.092 tons of carbon and in April 2023 for the SWR model, with a total of 0.091 tons of carbon. The monthly average of seagrass AGC based on the RFR is 17.85gC/m² for the Ea class, 11.90gC/m² for the EaTh class and 5.76gC/m² for the ThCr class. For SWR, the average is 18.83gC/m² for the Ea class, 8.03gC/m² for the EaTh class and 5.73gC/m² for the ThCr class. The average total AGC for 15 months, based on RFR, is 0.04 tons for the Ea class, 0.01 tons for the EaTh class and 0.05 tons for the ThCr class. The SWR indicates that the average total AGC is 0.04 tons for the Ea class, 0.005 tons for the EaTh class and 0.05 tons for the ThCr class. These results demonstrate that there are no significant differences in AGC across all species composition classes in both regression models.

Each species composition class exhibits different estimates of the highest and lowest AGC. Among these, the Ea class demonstrates a more consistent pattern of AGC dynamics compared

to other species composition classes. This stability can be attributed to several factors, including robust root systems, superior storage capacity, resistance to environmental stress, consistent growth and effective vegetative reproduction. These characteristics enable large seagrass species, such as Ea, to maintain more stable AGC dynamics [61]. In contrast, smaller seagrass species generally respond more rapidly to environmental changes and exhibit faster growth rates [61]. However, their smaller size also makes them more susceptible to environmental fluctuations, resulting in more variable seagrass biomass dynamics compared to larger species [62]. This variability is evident in the multitemporal AGC dynamics pattern of the ThCr class, which is more dynamic than the relatively stable Ea class.

The AGC dynamics pattern for the EaTh class appears consistent in the RFR model, but unstable in the SWR model. The EaTh class, representing all species on Pari Island, typically exhibits stable monthly biomass dynamics [63]. This class comprises various-sized seagrasses, forming a complex composition. Smaller seagrasses, such as ThCr, tend to dominate certain areas more rapidly under optimal conditions, while larger seagrasses provide long-term stability [62]. The different seagrass species complement each other in terms of ecosystem functions, including carbon sequestration, environmental stress tolerance and nutrient cycling. Consequently, fluctuations in seagrass AGC may be mitigated as some species continue to function optimally under changing conditions, thereby reducing large variations in total carbon stocks. The significant difference in EaTh class AGC dynamics between the RFR and SWR models may be attributed to SWR's limited capability in mapping AGC. The SWR model's simpler variable selection approach and assumption of linearity result in a failure to capture the complex dynamics present in the data, in comparison to the RFR model [64]. This results in the AGC dynamics of the SWR model being lower and more variable than those of the RFR model for the EaTh species composition class.

Figures 11 and 12 illustrate the AGC map for the 15 median composite Sentinel-2A images from April 2021 to December 2023.

These maps reveal monthly variations and dynamics in AGC changes. The seagrass AGC map derived from the RFR method exhibits more pronounced dynamics, as indicated by its diverse color gradations each month. In contrast, multitemporal AGC maps based on the SWR method display more monotonous color gradations. Specifically, the SWR-based maps predominantly show darker color gradations along the west and south coasts of Pari Island. Additionally, the species composition of the Ea and EaTh classes in the SWR-based AGC maps demonstrates less variation in color gradation. It is noteworthy that the EaTh class exhibits changes in color gradation in the eastern part of Pari Island, which indicates AGC dynamics in that region.

From June 2021 to August 2021, there was an increase in the AGC estimates for the Ea and ThCr classes. However, in October 2021, the AGC estimate for the Ea class decreased before increasing again in March 2022. The AGC dynamics for the RFR model are further illustrated in the AGC map from November 2022 to April 2023, which indicates a rise in AGC estimates. Both models demonstrate a decline in AGC estimates from March 2022 to August 2022, coinciding with the onset of the dry season. August is the driest month, as indicated in [59].

The resulting multitemporal AGC maps demonstrate that Sentinel-2 imagery is generally effective for AGC mapping and multitemporal analysis. Utilizing monthly median composites helps mitigate disturbances such as cloud cover or noise [33]. However, even with median composites, Sentinel-2 imagery does not consistently provide high-quality data, as evidenced by the anomaly in the multitemporal AGC results for January. Additionally, RFR and SWR models can effectively and consistently capture AGC dynamics. Although the results indicated that the RFR model generally performs better, this superiority may not apply to all months. The SWR model could be preferable in specific months, considering that the variations in multitemporal AGC maps from RFR and SWR are not significantly different.

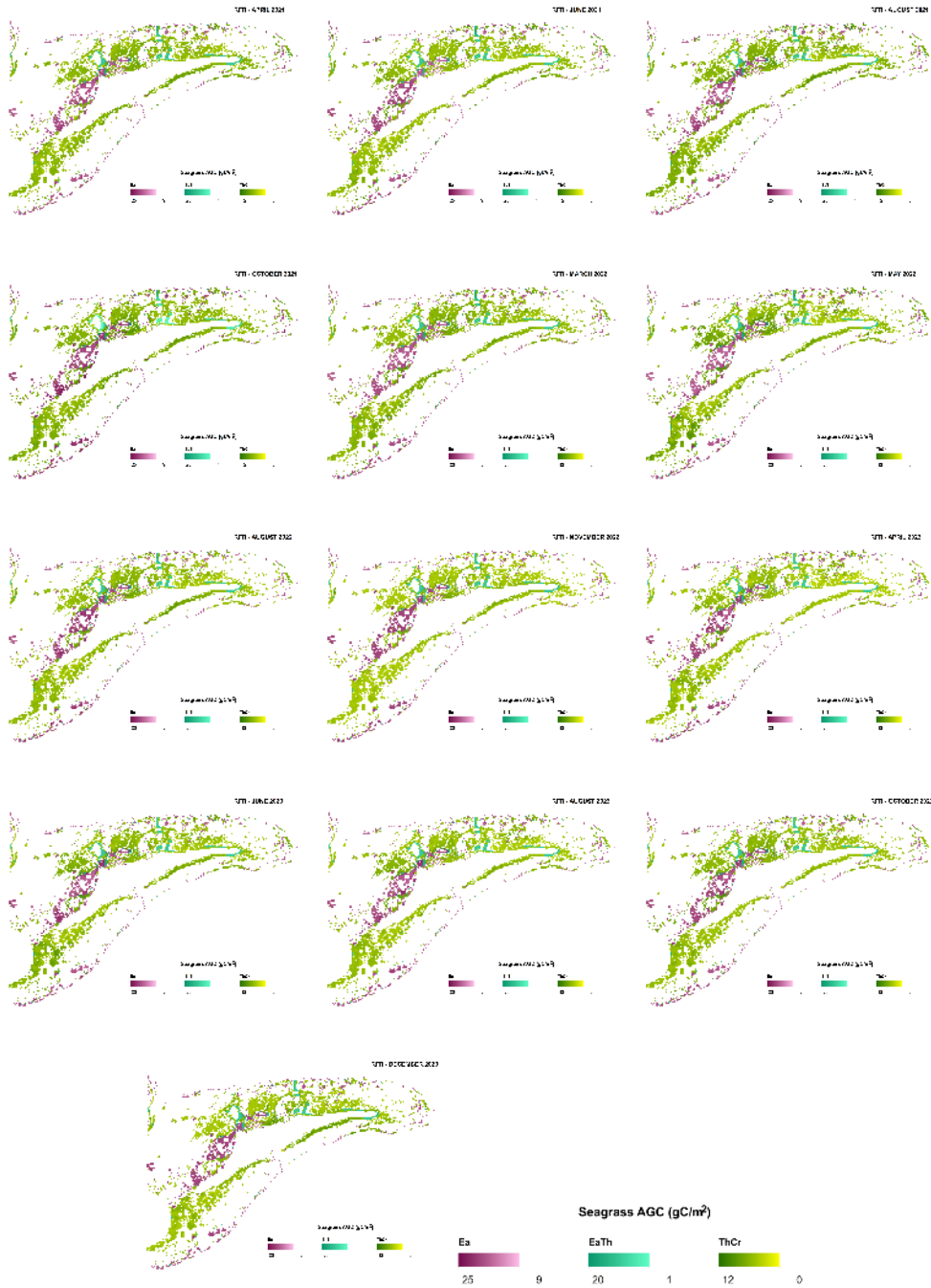


Fig. 11. Map of multitemporal seagrass AGC based on RFR

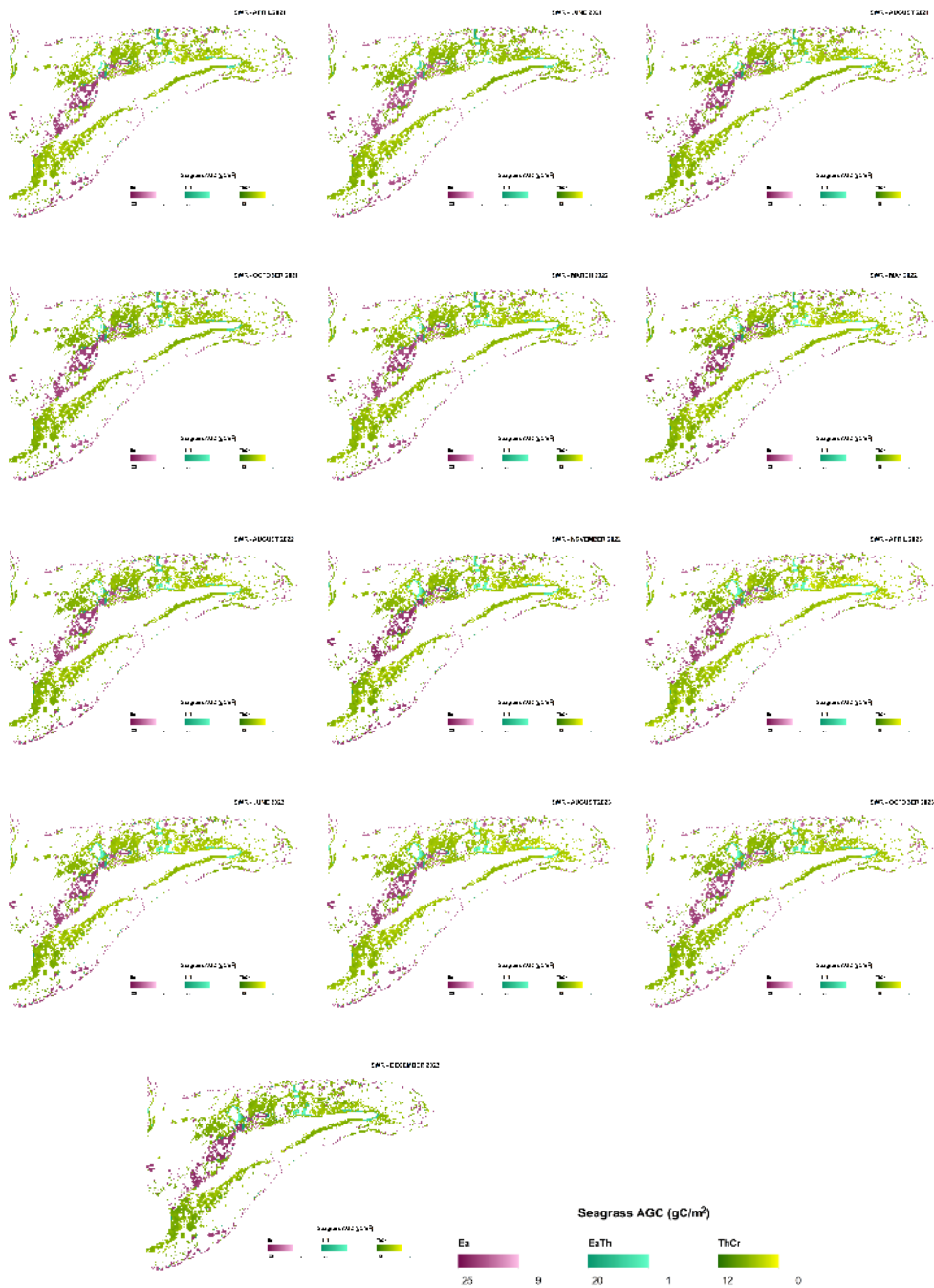


Fig. 12. Map of multitemporal seagrass AGC based on SWR

Environmental Factors Influencing Seagrass AGC dynamics

The dynamics of seagrass AGC are predominantly influenced by the growth and photosynthesis processes of seagrass. These processes are responsive to environmental fluctuations, including changes in temperature, salinity and chlorophyll concentration [44].

Furthermore, various factors impact seagrass AGC dynamics, such as the availability of sunlight, rainfall patterns and nutrient levels [65]. The seasonal fluctuations in seawater pH, which range from acidic to alkaline, serve as indicators of seagrass presence and growth [66]. Furthermore, chlorophyll concentration serves as a marker for identifying eutrophication [44]. In this study, pH value and chlorophyll concentration are the biochemical variables utilised for correlation analysis with AGC dynamics, while rainfall, sea surface temperature and salinity are the physical variables considered for analysis.

The data presented in Table 8 indicates rainfall exhibit significant correlations with seagrass AGC. However, not all classes of species composition display significant correlations between AGC and the environmental factors under consideration. For instance, the AGC from the RFR model and the AGC of the Ea class from the SWR model does not show a significant correlation with any of the factors examined. The strongest correlation is observed in the rainfall variable, with a correlation coefficient of 0.696 for the AGC of ThCr class from SWR model. Rainfall is an environmental factor affecting the availability of light and seawater temperature related to seagrass growth [65]. When rainfall increases, light and seawater temperatures will decrease due to increased cloud cover and sediment suspension that can rise due to terrestrial runoff.

Table 8. Correlation analysis results between seagrass AGC dynamics and environmental factors.

Environmental Factors	RFR			SWR		
	Ea	EaTh	ThCr	Ea	EaTh	ThCr
<i>pH</i>	-0.465	0.081	0.353	-0.216	0.097	-0.163
Chlorophyll	-0.511	0.380	0.343	-0.024	0.144	-0.218
Rainfall	0.417	0.086	-0.127	0.527	0.665*	0.696*
Salinity	0.361	0.174	-0.117	0.290	0.197	0.176
<i>Sea Surface Temperature (SST)</i>	0.047	0.093	-0.178	0.108	0.025	-0.067

*Significant at 0.05

Figure 13 shows a comparison graph between the multitemporal mean AGC and biophysical variables. Based on the graph, the relationship between AGC and pH (Fig. 13a), chlorophyll concentration (Fig. 13b), SST (Fig. 13c) and salinity (Fig. 13d) is less visible. The correlation results show that only the rainfall variable has a correlation with the multitemporal AGC. This can be seen from the pattern shown in the comparison graph of AGC and rainfall (Fig. 13e). The rainfall variable shows a reasonably high influence on seagrass AGC, where most of the average seagrass AGC follows the dynamic rainfall pattern. The highest rainfall was in December 2023 and seagrass AGC also increased. However, this is inappropriate with a general dynamic pattern of AGC because, usually, the AGC decreases when rainfall is too high, as shown by the AGC class Ea for the RFR model. This anomaly is caused by inconsistent image quality due to disturbances like cloud cover or fog.

Although other biophysical variables did not show a significant correlation with multitemporal AGC data, biophysical variables such as pH, chlorophyll concentration, salinity and SST can generally affect seagrass AGC dynamics [65-68]. Several factors cause the correlation between these biophysical variables and the modeled multitemporal AGC data to be less significant. Some include temporal and spatial variations, complex interactions between influential factors and various seagrass species [69-73]. Spatial and temporal variations in biophysical parameters, such as slight differences between SST data collection stations, may affect the correlation with seagrass AGC data. Variability in seagrass AGC may occur on such a small scale that it is not captured in the sampling design [71-73]. In addition, seagrasses need time to respond to changes in biophysical variables. It is possible that measurements of

biophysical variables were taken at a different time than seagrass AGC measurements or there was a lag time in response. So, less representative sampling can lead to less significant results.

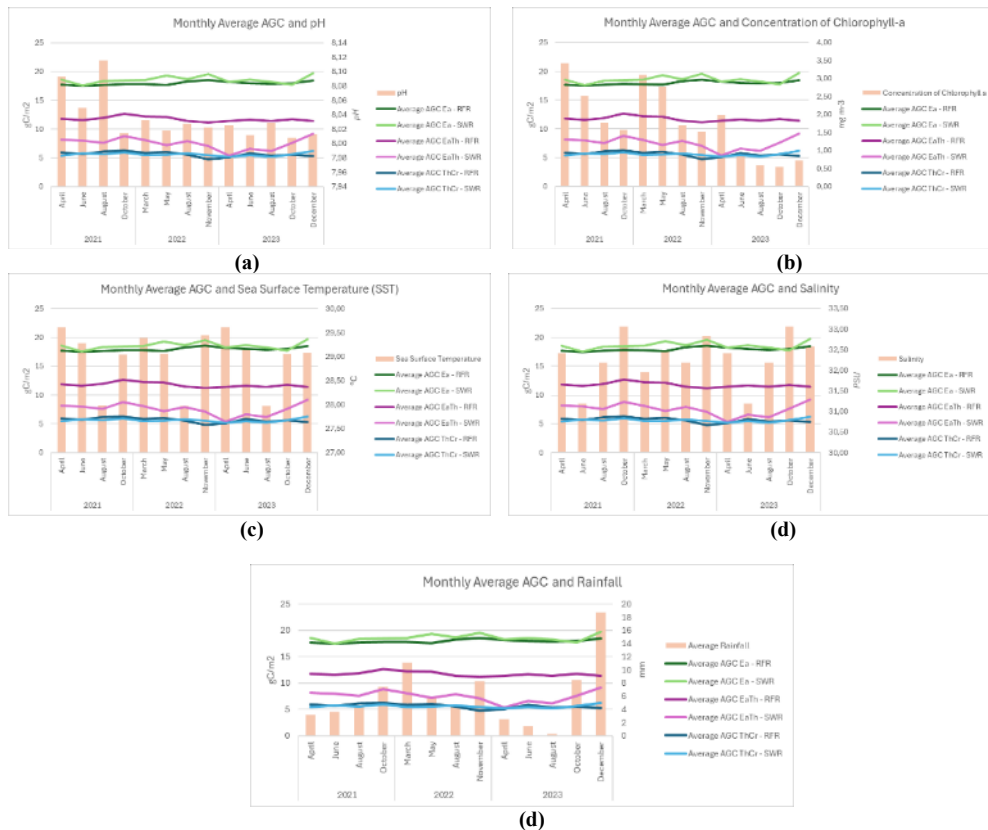


Fig. 13. Map of Multitemporal Seagrass AGC based on Stepwise Regression

The complex interactions between each biophysical variable and various seagrass species and other factors, such as external disturbances, can affect the correlation results with AGC data [71, 73]. Seagrass ecosystems are complex systems with many interactions between biotic and abiotic variables. Biophysical variables such as salinity, pH, chlorophyll concentration and temperature can be influenced by various other unmeasured or uncontrollable variables. In addition, different seagrass species have different storage capacities and responses to environmental conditions [44]. Some seagrass species are more resistant to environmental changes, so fluctuations in biophysical variables may not be directly visible in seagrass AGC [74]. Heterogeneity in seagrass communities can make it difficult to see relationships between biophysical variables and seagrass AGC by species composition class.

Importance of Seagrass Time Series for Conservation

Monitoring the seagrass PC and AGC is necessary for comprehending changes and undertaking carbon inventories. Seagrasses exert a significant global influence by bolstering food security, mitigating climate change and fostering biodiversity [70, 75]. Despite conservation efforts, seagrass meadows face mounting pressures from both natural forces and human activities, resulting in degradation and functional loss [76]. The implementation of effective management strategies is of paramount importance if seagrass coverage is to be restored and their pivotal role in coastal marine ecosystems is to be amplified. One such strategy is the establishment of

conservation zones [68]. The maintenance of up-to-date information on seagrass PC and AGC is essential if efficacious and sustainable conservation efforts are to be ensured and if global climate change challenges are to be addressed. Maps delineating seagrass PC and AGC assist in the evaluation of the health of seagrass ecosystems. The implementation of continuous monitoring enables the early detection of any changes or degradation to the habitat, which is highly important for the prompt implementation of conservation interventions [77].

The determination of conservation areas can be facilitated by utilizing the coefficient of variation (CV) values derived from multitemporal AGC maps. In order to identify locations on Pari Island characterised by relatively stable AGC levels, an analysis of AGC coefficient of variation was conducted. A higher coefficient of variation indicates greater temporal variability in seagrass AGC. Variations exceeding 30% are deemed less suitable for inclusion in conservation areas [78]. Such high variations, whether resulting from natural causes such as disasters or human activities, have the potential to disrupt natural habitats. Conservation areas necessitate stable ecosystems to uphold robust biodiversity and ensure the survival of protected species. Frequent fluctuations can upset ecosystem equilibrium and pose threats to the species inhabiting them. Moreover, excessive environmental variation can hinder the ability of some species to adapt swiftly, thereby elevating the risk of local extinction [79].

The analysis of the resulting CV map reveals that a significant portion of the seagrass cover on Pari Island is suitable for conservation purposes (Fig. 14). When examining the CV map derived from time-series seagrass AGC maps, it becomes evident that the highest values are attributed to the Ea class at 31%, the EaTh class at 24% and the ThCr class at 37% over a span of 15 months. This distribution of CV values indicates that the EaTh species composition class exhibits a comparatively higher level of stability, as evidenced by its CV range remaining below 30%. It is noteworthy that different species of seagrass respond diversely to environmental factors such as temperature, salinity and nutrient availability [63]. Consequently, areas covered by various species can mitigate the overall variability of carbon stocks. This is due to the likelihood that certain species will continue to function optimally despite changing conditions, thus minimizing the occurrence of strong fluctuations in the AGC.

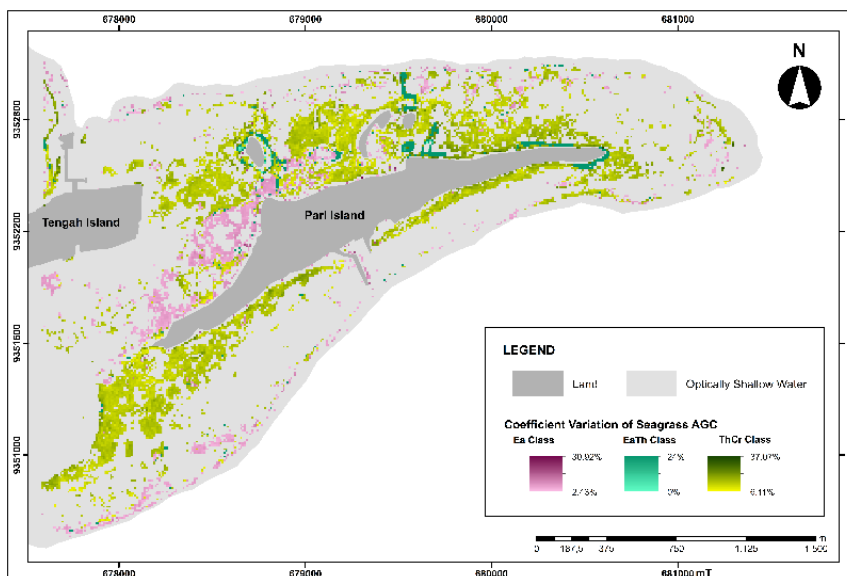


Fig. 14. Coefficient of variation (CV) map based on multitemporal seagrass AGC maps. Lower values indicate stable seagrass AGC across 2021-2023 and vice versa

The ThCr class exhibits greater variation than the Ea class, largely due to differing responses to environmental changes. The ThCr class typically exhibits faster growth rates but is also more vulnerable to fluctuations in environmental conditions [80]. Conversely, the large-size Ea species demonstrate slower growth rates but greater resilience to drastic changes [81]. Although the maximum CV exceeding 30% for both the Ea and ThCr classes exists, most seagrass areas maintain values below 30%. Higher CV values are observed in areas closer to the mainland along the coast. Consequently, alongside the environmental factors influencing seagrass dynamics, human accessibility can impact the stability of seagrass AGC. This is because seagrasses situated in close proximity to the shoreline may be subjected to heightened exposure to anthropogenic influences or competition for growth with algae [82].

Conclusions

A mapping model for seagrass AGC at the species composition level, utilizing Sentinel-2 images, has been successfully developed. The results demonstrated that the RFR model exhibited greater accuracy in AGC mapping compared to the SWR model. When applied to multitemporal AGC mapping on Pari Island, the RFR-based model revealed average monthly AGC values of 17.85gC/m² for the Ea class, 11.90gC/m² for the EaTh class and 5.76gC/m² for the ThCr class. Conversely, the SWR-based model yielded average AGC values of 18.83 gC/m² for the Ea class, 8.03gC/m² for the EaTh class and 5.73gC/m² for the ThCr class, which were relatively comparable to the RFR results. However, certain multitemporal AGC map outputs, notably those from January, were deemed unrepresentative due to poor image quality. This anomaly in AGC dynamics can be attributed to the varying quality of images used over a 15-month period, which impacted the reflectance values. Furthermore, external factors such as rainfall also influence AGC dynamics. Higher rainfall is generally associated with increased AGC estimates, as observed in December 2023. Finally, the low CV of AGC across all species composition classes indicates that most of the seagrass areas on Pari Island are suitable for conservation efforts.

Acknowledgments

This research was funded through the 2024 Final Project Recognition Program from the Faculty of Geography, Universitas Gadjah Mada. The research entitled "Development of a Model for Mapping the Dynamics of Aboveground Carbon Stocks of Seagrass Ecosystems on Pari Island and Menjangan Besar Island Using Sentinel-2 Integration and Artificial Intelligence Algorithms" has been authorized through letter number 4971/UN1.P1/PT.01.01/2024 dated April 30, 2024.

References

- [1] * * *, UNFCCC, **Caring for Climate: A Guide to the Climate Change Convention and the Kyoto Protocol**, Revised 2005 ed, Bonn, Germany, 2005, [Online]. Available: <https://library.sprep.org/content/caring-climate-guide-climate-change-convention-and-kyoto-protocol-0>.
- [2] A. Lawrence, **Blue Carbon**, Jakarta, 2013.
- [3] N. Nawari, A. Syahza, Y.I. Siregar, *Community-based mangrove forest management as ecosystem services provider for reducing CO₂ emissions with carbon credit system in Bengkalis District, Riau, Indonesia*, **Journal of Physics Conference Series**, **2049**(1), 2021, Article Number: 012074. DOI: 10.1088/1742-6596/2049/1/012074.
- [4] N. Zurba, **Pengenalan Padang Lamun Suatu Ekosistem yang Terlupakan**, Lhokseumawe: Unimal Press, 2018.
- [5] N.D.M. Sjafrie *et al.*, **Status padang lamun Indonesia 2018**, Jakarta, 2018.
- [6] J. Fourqurean *et al.*, **Coastal Blue Carbon: Methods for Assessing Carbon Stocks and**

- Emissions Factors in Mangroves, Tidal Salt Marshes, and Seagrasses.** Conservation International, Intergovernmental Oceanographic Commission of UNESCO, International Union for Conservation of Nature, 2014. [Online]. Available: <https://www.unep.org/resources/publication/coastal-blue-carbon-methods-assessing-carbon-stocks-and-emissions-factors>.
- [7] D. Deyanova, M. Gullström, L.D. Lyimo, M. Dahl, M.I. Hamisi, M.S.P. Mtolera, M. Björk., *Contribution of seagrass plants to CO₂ capture in a tropical seagrass meadow under experimental disturbance*, **PLoS One**, **12**(7), 2017, Article Number: e0181386. DOI: 10.1371/journal.pone.0181386.
- [8] A.M. Tamondong, C. Cruz, R.R. Quides, M. Garcia, J.A. Cruz, J. Guihawan, A. Blanco, *Remote sensing-based estimation of seagrass percent cover and LAI for above ground carbon sequestration mapping*, **Remote Sensing of the Open and Coastal Ocean and Inland Waters**, **10778**, 2018, Article Number: UNSP 1077803. DOI: 10.1117/12.2324695.
- [9] A.J. Wahyudi, S. Rahmawati, A. Irawan, H. Hadiyanto, B. Prayudha, M. Hafizt, A. Afdal, N.S. Adi, A. Rustam, U.E. Hernawan, Y.P. Rahayu, M.Y. Iswari, I.H. Supriyadi, T. Solihudin, R.N.A. Ati, T.L. Kepel, M.A. Kusumaningtyas, A. Daulat, H.L. Salim, N. Sudirman, D.D. Suryono, W. Kiswara, *Assessing Carbon Stock and Sequestration of the Tropical Seagrass Meadows in Indonesia*, **Ocean Science Journal**, **55**(1), 2020, pp. 85-97.
- [10] H. Kennedy, M. Bjork, *Seagrass Meadows*, in: **The Management of Natural Coastal Carbon Sinks Edited by Dan Laffoley and Gabriel Grimsditch**, Gland, Switzerland: IUCN, 2009, pp. 23-30 [Online]. Available: www.iucn.org/marine.
- [11] FR. Gell, M. W. Whittington, *Diversity of fishes in seagrass beds in the Quirimba Archipelago, northern Mozambique*, **Mar. Freshw. Res.**, **53**, pp. 115-121, 2002.
- [12] H. Latuconsina, M. Nessa, R.A. Rappe, *Komposisi spesies dan struktur komunitas ikan padang lamun di Perairan Tanjung Tiram – Teluk Ambon Dalam*, **Journal Ilmu dan Teknol. Kelaut. Trop.**, **4**(1), 2012, pp. 35-46.
- [13] P.T. Harris, E.K. Baker, **Why Map Benthic Habitats?** Sydney, Elsevier, 2012. DOI: 10.1016/B978-0-12-385140-6.00001-3.
- [14] P. Wicaksono, M. Hafizt, *Mapping seagrass from space: Addressing the complexity of seagrass LAI mapping*, **European Journal of Remote Sensing**, **46**(1), 2013, pp. 18-39. DOI: 10.5721/EuJRS20134602.
- [15] S.M. Hamylton, **Spatial Analysis of Coastal Environments**, 2017, Taylor&Francis, DOI: 10.1080/2325548x.2018.1508194.
- [16] M.A. Fauzan, I.S.W. Kumara, R.N. Yogyantoro, S.W. Suwardana, N. Fadhilah, I. Nurmalasari, S. Apriyani, P. Wicaksono, *Assessing the capability of sentinel-2A data for mapping seagrass percent cover in Jerowaru, East Lombok*, **Indonesian Journal of Geography**, **49**(2), 2017, pp. 195-203. DOI: 10.22146/ijg.28407.
- [17] P. Wicaksono, P. Danoedoro, Hartono, U. Nehren, A. Maishella, M. Hafizt, S. Arjasakusuma, S.D. Harahap, *Analysis of field seagrass percent cover and aboveground carbon stock data for non-destructive aboveground seagrass carbon stock mapping using worldview-2 image*, **International Archives of the Photogrammetry, Remote Sensing and Spatial Information Sciences**, **46**(4), 2021, Article Number: W6-2021, pp. 321-327. DOI: 10.5194/isprs-Archives-XLVI-4-W6-2021-321-2021.
- [18] M.S. Hossain, J.S. Bujang, M.H. Zakaria, M. Hashim, *The application of remote sensing to seagrass ecosystems: an overview and future research prospects*, **International Journal of Remote Sensing**, **36**(1), 2015, pp. 61-113. DOI: 10.1080/01431161.2014.990649.
- [19] M. Lyons, C. Roelfsema, E. Kovacks, J. Samper-Villarreal, M. Saunders, P. Paxwell, S. Phinn, *Rapid monitoring of seagrass biomass using a simple linear modelling approach , in the field and from space*, **Marine Ecology Progress Series.**, **530**, 2015, pp. 1-14. DOI: 10.3354/meps11321.
- [20] C.M. Roelfsema, E.M. Kovacs, S.R. Phinn, *Field Data Sets for Seagrass Biophysical*

- Properties for the Eastern Banks, Moreton Bay, Australia, 2004-2014*, **Scientific Data**, **2**, 2015, Article Number: 150040. DOI: 10.1038/sdata.2015.40.
- [21] M.D. Fortes, J.L.S. Ooi, Y.M. Tan, A. Prathep, J.S. Bujang, S.M. Yaakub, *Seagrass in Southeast Asia: A review of status and knowledge gaps, and a road map for conservation*, **Botanica Marina**, **61**(3), 2018, pp. 269-288. DOI: 10.1515/bot-2018-0008.
- [22] * * *, UNEP, **Out of the Blue the Value of Seagrasses**, 2020.
- [23] M.N. Akbar, A. Faizal, Y.A. La Nafie, S. Werorilangi, S. Mashoreng, *Seagrass carbon stock estimation in Panrangluhu coastal waters using remote sensing technology*, **IOP Conference Series. Earth Environmental Science**, **860**, 2021, Article Number: 012085. DOI: 10.1088/1755-1315/860/1/012085.
- [24] A.J. Wahyudi, B. Prayudha, M. Hafitz, L.O. Alifatri, U.E. Hernawan, A. Salatalohi, F. Febriani, *Introducing a Method for Calculating Carbon Emission Reduction on the Seagrass Ecosystem for Indonesia's Low Carbon Development Initiative*, **IOP Conference Series. Earth Environmental Science**, **789**(1), 2021, Article Number: 012014. DOI: 10.1088/1755-1315/789/1/012014.
- [25] J.D. Hedley, B.J. Russell, K. Randolph, M.A. Perez-Castro, R.M. Vasquez-Elizondo, S. Enriquez, H.M. Dierssen, *Remote Sensing of Seagrass Leaf Area Index and Species: The Capability of a Model Inversion Method Assessed by Sensitivity Analysis and Hyperspectral Data of Florida Bay*, **Frontiers in Marine Science**, **4**, 2017, Article Number: 362. DOI: 10.3389/fmars.2017.00362.
- [26] R.W. Shafiya, A. Djunaedi, R. Ario, *Estimasi Biomassa dan Simpanan Karbon pada Vegetasi Lamun di Perairan Pantai Jepara*, **Journal of Marine Research**, **10**(3), 2021, pp. 446-452. DOI: 10.14710/jmr.v10i3.30998.
- [27] M.A. Fauzan, P. Wicaksono, Hartono, *Characterizing Derawan Seagrass Cover Change with Time-Series Sentinel-2 Images*, **Regional Studies in Marine Science**, **48**, 2021, Article Number: 102048, DOI: 10.1016/j.rsma.2021.102048.
- [28] P. Wicaksono, S.A. Wulandari, W. Lazuardi, M. Munir, *Sentinel-2 Images Deliver Possibilities for Accurate and Consistent Multi-Temporal Benthic Habitat Maps in Optically Shallow Water*, **Remote Sensing Applications - Society and Environmental**, **23**, 2021, Article Number: 100572. DOI: 10.1016/j.rsase.2021.100572.
- [29] M. Rais, D.F. Inaku, W.J.C. Moka, S. Mashoreng, D.Y. Satari, N. Rukminasari, *Estimasi Stok Karbon Padang Lamun menggunakan Citra Spot-7 di Perairan Pulau Kodingarenglombo, Sangkarrang, Kota Makassar*, **J. Kelaut. Trop.**, **26**(2), pp. 387-398, 2023.
- [30] M.D.M. Manessa, M. Haidar, S. Budhiman, G. Winarso, A. Kanno, T. Sagawa, M. Sekine, *Evaluating the Performance of Lyzenga's Water Column Correction in Case-1 Coral Reef Water using a Simulated Wolrdview-2 Imagery*, **IOP Conference Series. Earth Environmental Science**, **47**, 2016, Article Number: 012018, DOI: 10.1088/1755-1315/47/1/012018.
- [31] A. Rustam, *Pemantauan Ekosistem Lamun Pulau Pari Dan Pulau Tikus Monitoring of Seagrass Ecosystem At Pari Island and Tikus Island*, **J. Ris. Jakarta**, **12**(1), pp. 7-15, 2019.
- [32] R. Rochmady, *Rehabilitasi Ekosistem Padang Lamun*, **SSRN Electron. Journal**, 2010, pp. 1-25, DOI: 10.2139/ssrn.3045214.
- [33] N. Flood, *Seasonal composite landsat TM/ETM+ Images using the medoid (a multi-dimensional median)*, **Remote Sensing**, **5**(12), pp. 6481-6500, 2013, DOI: 10.3390/rs5126481.
- [34] A.W. Hastuti, K.I. Suniada, M. Nagai, *Detection of Coastline Changes using Multi-Temporal Satellite Images: A case study of Gianyar and Klungkung Regency, Bali*, **IOP Conference Series. Earth Environmental Science**, **1095**(1), 2022, DOI: 10.1088/1755-1315/1095/1/012003.
- [35] C. Roelfsema, S. Phinn, **A Manual for Conducting Georeferenced Photo Transects Surveys to Assess the Benthos of Coral Reef and Seagrass Habitats**, Brisbane, Australia,

- 2009.
- [36] P. Wicaksono, M.A. Fauzan, I.S.W. Kumara, R.N. Yogyantoro, W. Lazuardi, Z. Zhafarina, *Analysis of reflectance spectra of tropical seagrass species and their value for mapping using multispectral satellite images*, **International Journal of Remote Sensing**, **40**(23), 2019, pp. 8955-8978. DOI: 10.1080/01431161.2019.1624866.
- [37] L. Breiman, *Random Forest*, **Machine Learning**, **45**(1), 2001, pp. 5-32. DOI: 10.1023/A:1010933404324.
- [38] N.K. Dewi, S.Y. Mulyadi, U.D. Syafitri, *The Application of Random Forest in Driver Analysis*, **Forum Statistika dan Komputasi**, **16**(1), 2011, pp. 35-43.
- [39] E. Scornet, *Trees, Forests, and Impurity-Based Variable Importance in Regression*, **Annales de l'Institut Henri Poincaré - Probabilités et Statistiques**, **59**(1), pp. 1-40, 2021, DOI: 10.1214/21-aihp1240.
- [40] I. Reis, D. Baron, S. Shahaf, *Probabilistic Random Forest: A Machine Learning Algorithm for Noisy Data Sets*, **Astronomical Journal**, **157**(1), 2018, Article Number: 16, DOI: 10.3847/1538-3881/aaf101.
- [41] P. Wicaksono, A. Maishella, A.J. Wahyudi, M. Hafizt, *Multitemporal seagrass carbon assimilation and aboveground carbon stock mapping using Sentinel-2 in Labuan Bajo 2019–2020*, **Remote Sensing Applications - Society and Environmental**, **27**, 2022, Article Number: 00803. DOI: 10.1016/j.rsase.2022.100803.
- [42] R.R. Hocking, *A Biometrics Invited Paper. The Analysis and Selection of Variables in Linear Regression*, **Biometrics**, **32**(1), 1976, pp. 1-49. DOI: 10.2307/2529336.
- [43] N.R. Draper, H. Smith, **Applied Regression Analysis**, Third Edit. New York: John Wiley & Sons, 1998. DOI: 10.2307/1401351.
- [44] B.K. Veettil, R.D. Ward, M.D.A.C. Lima, M. Stankovic, P.N. Hoai, N.X. Quang, *Opportunities for seagrass research derived from remote sensing: A review of current methods*, **Ecological Indicators**, **117**, 2020, DOI: 10.1016/j.ecolind.2020.106560.
- [45] C. Funk, P. Peterson, M. Landsfeld, D. Pedreros, J. Verdin, S. Shukla, G. Husak, J. Rowland, L. Harrison, A. Hoell, J. Michaelsen, *The climate hazards infrared precipitation with stations - A new environmental record for monitoring extremes*, **Scientific Data**, **2**, 2015, Article Number: 150066. DOI: 10.1038/sdata.2015.66.
- [46] * * *, European Union, **Copernicus: Europe's Eye on Earth**, Brussels, 2015. DOI: 10.2873/93104.
- [47] P. Wicaksono, W. Lazuardi, *Assessment of PlanetScope images for benthic habitat and seagrass species mapping in a complex optically shallow water environment*, **International Journal of Remote Sensing**, **39**(17), 2018, pp. 5739-5765. DOI: 10.1080/01431161.2018.1506951.
- [48] A. Ariasari, Hartono, P. Wicaksono, *Random forest classification and regression for seagrass mapping using PlanetScope image in Labuan Bajo, East Nusa Tenggara*, **Sixth International Symposium on LAPAN-IPB Satellite**, **11372**, 2019, DOI: 10.1117/12.2541718
- [49] P. Wicaksono, M.A. Fauzan, S.G.W. Asta, *Assessment of Sentinel-2A multispectral image for benthic habitat composition mapping*, **IET Image Processing**, **14**(2), 2020, pp. 279-288, DOI: 10.1049/iet-ipr.2018.6044.
- [50] V. Gouldsmith, A. Cooper, *Consideration of the carbon sequestration potential of seagrass to inform recovery and restoration projects within the Essex Estuaries Special Area of Conservation (SAC), United Kingdom*, **Journal of Coastal Conservation**, **26**(4), 2022, pp. 1-21. DOI: 10.1007/s11852-022-00882-3.
- [51] P. Wicaksono, A. Maishella, S. Arjasakusuma, W. Lazuardi, S.D. Harahap, *Assessment of WorldView-2 images for aboveground seagrass carbon stock mapping in patchy and continuous seagrass meadows*, **International Journal of Remote Sensing**, **43**(8), 2022, pp. 2915-2941. DOI: 10.1080/01431161.2022.2074809.

- [52] P. Wicaksono, I.S.W. Kumara, M. Kamal, M.A. Fauzan, Z. Zhafarina, D.A. Nurswantoro, R.N. Yogyantoro, *Multispectral Resampling of Seagrass Species Spectra: WorldView-2, Quickbird, Sentinel-2A, ASTER VNIR, and Landsat 8 OLI*, **IOP Conference Series. Earth Environmental Science**, **98**(1), 2017, Article Number: 012039. DOI: 10.1088/1755-1315/98/1/012039.
- [53] J. Rui, H. Zhang, D. Zhang, F. Han, Q. Guo, *Total organic carbon content prediction based on support-vector-regression machine with particle swarm optimization*, **Journal of Petroleum Science and Engineering**, **180**, 2019, pp. 699-706. DOI: 10.1016/j.petrol.2019.06.014.
- [54] M. C. Lebrasse et al., *Temporal Stability of Seagrass Extent, Leaf Area, and Carbon Storage in St. Joseph Bay, Florida: a Semi-automated Remote Sensing Analysis*, **Estuaries and coasts: Journal of the Estuarine Research Federation**, **45**, 2022, pp. 2082-2101. DOI: 10.1007/s12237-022-01050-4.
- [55] P. Zhao, D. Lu, G. Wang, C. Wu, Y. Huang, S. Yu, *Examining spectral reflectance saturation in landsat imagery and corresponding solutions to improve forest aboveground biomass estimation*, **Remote Sensing**, **8**(6), 2016, DOI: 10.3390/rs8060469.
- [56] P. Wicaksono, M.A. Fauzan, I.S.W. Kumara, R.N. Yogyantoro, W. Lazuardi, Z. Zhafarina, *Analysis of Reflectance Spectra of Tropical Seagrass Species and Their Value for Mapping using Multispectral Satellite Images*, **International Journal of Remote Sensing**, **40**(23), 2019, pp. 8955-8978. DOI: 10.1080/01431161.2019.1624866.
- [57] S. Mashoreng, Y.A.L. Nafie, B. Selamat, R. Isyrini, K. Amri, *Changes in seagrass carbon stock: Implications of decreasing area and percentage cover of seagrass beds in Barranglombo Island, Spermonde archipelago, South Sulawesi, Indonesia*, **IOP Conference Series. Earth Environmental Science**, **763**(1), 2021, Article Number: 012014. DOI: 10.1088/1755-1315/763/1/012014.
- [58] I. Mazarrasa, J. Samper-Villarreal, O. Serrano, P.S. Lavery, C.E. Lovelock, N. Marba, C.M. Duarte, J. Cortes, *Habitat characteristics provide insights of carbon storage in seagrass meadows*, **Marine Pollution Bulletin**, **134**, 2018, pp. 106-117. DOI: 10.1016/j.marpolbul.2018.01.059.
- [59] B. P. Statistik, **Statistik Daerah Kepulauan Seribu 2022**, Jakarta: Badan Pusat Statistik Kabupaten Kepulauan Seribu, 2022.
- [60] S. Diposaptono, Budiman, F. Agung, **Menyiasati Perubahan Iklim Di Wilayah Pesisir dan Pulau-pulau Kecil**, 2013. [Online]. Available: <https://surajis.files.wordpress.com/2017/12/menyiasati-perubahan-iklim-di-wp3k.pdf>
- [61] G.A. Juma, A.M. Magana, G.N. Michael, J.G. Kairo, *Variation in Seagrass Carbon Stocks Between Tropical Estuarine and Marine Mangrove-Fringed Creeks*, **Frontiers in Marine Science**, **7**, 2020, pp. 1-11. DOI: 10.3389/fmars.2020.00696.
- [62] V.M.N.C.S. Vieira, I.E. Lopes, J.C. Creed, *A model for the biomass-density dynamics of seagrasses developed and calibrated on global data*, **BMC Ecology**, **19**(1), 2019, Article Number: 4. DOI: 10.1186/s12898-019-0221-4.
- [63] B.J. Cardinale, J.E. Duffy, A. Gonzalez, D.U. Hooper, C. Perrings, P. Venail, A. Narwani, G.M. Mace, d. Tilman, D.A. Wardle, A.P. Kinzig, G.C. Daily, M. Loreau, J.B. Grace, A. Larigauderie, D.S. Srivastava, S. Naem, *Biodiversity loss and its impact on humanity*, **Nature**, **486**, 2012, pp. 59-67. DOI: 10.1038/nature11148.
- [64] I. Farooq, S.A. Bangroo, O. Bashir, T.I. Shah, A.A. Malik, A.M. Iqbal, S.S. Mahdi, O.A. Wani, N. Nazir, A. Biswas, *Comparison of Random Forest and Kriging Models for Soil Organic Carbon Mapping in the Himalayan Region of Kashmir*, **Land**, **11**(12), Article 2022, Number: 2180. DOI: 10.3390/land11122180.
- [65] L.J. McKenzie, S.M. Yaakub, R. Tan, J. Seymour, R.L. Yoshida, *Seagrass habitats of Singapore: Environmental drivers and key processes*, **Raffles Bulletin of Zoology, Supplement 34**, Part: 1, 2016, pp. 60-77.

- [66] D. Ganguly, G. Singh, P. Ramachandran, A.P. Selvam, K. Banerjee, R. Ramachandran, *Seagrass metabolism and carbon dynamics in a tropical coastal embayment*, **Ambio**, **46**(6), 2017, pp. 667-679. DOI: 10.1007/s13280-017-0916-8.
- [67] B.W. Touchette, *Seagrass-salinity interactions: Physiological mechanisms used by submersed marine angiosperms for a life at sea*, **Journal of Experimental of Marine Biology and Ecology**, **350**(1-2), 2007, pp. 194-215. DOI: 10.1016/j.jembe.2007.05.037.
- [68] C.M. Duarte, T. Sintes, N. Marbà, *Assessing the CO₂ Capture Potential of Seagrass Restoration Projects*, **Journal of Applied Ecology**, **50**(6), 2013, pp. 1341-1349. DOI: 10.1111/1365-2664.12155.
- [69] V. Endarwantti, A. Djunaedi, G.W. Santosa, *Estimasi Simpanan Karbon dan Bioekologi Lamun di Pantai Prawean, Jepara*, **Journal of Marine Research**, **12**(4), 2023, pp. 579-585. DOI: 10.14710/jmr.v12i4.35699.
- [70] J.W. Fourqurean, C.M. Duarte, H. Kennedy, M. Kolmer, M.A. Mateo, E.T. Apostolaki, G.A. Kendrick, D. Krause-Jensen, K.J. McGalthery, O. Serrano, *Seagrass ecosystems as a globally significant carbon stock*, **Nature Geoscience**, **5**(7), 2012, pp. 505-509. DOI: 10.1038/ngeo1477.
- [71] B. Hamuna, R.H.R. Tanjung, S. Suwito, H.K. Maury, A. Alianto, *Study of Seawater Quality and Pollution Index Based on Physical-Chemical Parameters in the Waters of the Depapre District, Jayapura*, **Journal Ilmu Lingkungan**, **16**(1), 2018, pp. 35-43. DOI: 10.14710/jil.16.135-43.
- [72] A.H. Nugraha, I.A. Tasabaramo, U.E. Hernawan, S. Rahmawati, R.D. Putra, F. Idris, *Estimasi Stok Karbon Padaekosistem Lamun Di Perairan Utara Papua (Studi Kasus : Pulau Liki, Pulau Befondi Dan Pulau Meossu)*, **Jurnal of Kelautan Tropis**, **23**(3), 2020, pp. 291-298. DOI: 10.14710/jkt.v23i3.7939.
- [73] T. Repolho, B. Duarte, G. Dionisio, J.R. Paula, A.R. Lopes, I.C. Rosa, T.I. Grilo, I. Cacador, R. Calado, R. Rosa, *Seagrass ecophysiological performance under ocean warming and acidification*, **Scientific Report**, **7**, 2017, Article Number: 41443. DOI: 10.1038/srep41443.
- [74] C.F. Chen, V.K. Lau, N. Bin Chang, N.T. Son, P.H.S. Tong, S.H. Chiang, *Multi-temporal change detection of seagrass beds using integrated Landsat TM/ETM +/OLI imageries in Cam Ranh Bay, Vietnam*, **Ecology Informatics**, **35**, 2016, pp. 43-54. DOI: 10.1016/j.ecoinf.2016.07.005.
- [75] R.K.F. Unsworth, L.J. McKenzie, C.J. Collier, L.C. Cullen-Unsworth, C.M. Duarte, J.S. Eklóf, J.C. Jarvis, B.L. Jones, L.M. Nordlund, *Global challenges for seagrass conservation*, **Ambio**, **48**(8), 2019, pp. 801-815. DOI: 10.1007/s13280-018-1115-y.
- [76] S. Kuriandewa, T.E., Kiswara, W., Hutomo, M. Soemodihardjo, *The Seagrass on Indonesia*, **World Atlas of Seagrasses**, Berkeley: UNEP-WCMC by the University of California Press, 2003. DOI: 10.5860/choice.41-3160.
- [77] K.M. Tabor, M.B. Holland, *Opportunities for improving conservation early warning and alert systems*, **Remote Sensing in Ecology and Conservation**, **7**(1), 2021, pp. 7-17. DOI: 10.1002/rse2.163.
- [78] N. Dudley, S. Stolton, **Best Practice in Delivering the 30x30 Target: Protected Areas and Other Effective Area-Based Conservation Measures**, Report-Biodiversity Conservation, The Nature Conservancy-Equilibrium Research, UK, 2022.
- [79] J. Pazzaglia, T.B.H. Reusch, A. Terlizzi, L. Marín-Guirao, G. Procaccini, *Phenotypic plasticity under rapid global changes: The intrinsic force for future seagrasses survival*, **Evolutionary Applications**, **14**(5), 2021, pp. 1181-1201. DOI: 10.1111/eva.13212.
- [80] C.I. Tupan, P.A. Uneputty, *Growth and Production of Leaves Thalassia hemprichii on The Suli Coastal Waters, Ambon Island*, **International Journal of Marine Engineering and Innovation Research**, **2**(2), 2018, pp. 0-4. DOI: 10.12962/j25481479.v2i2.3647.
- [81] N. Marbà, C.M. Duarte, A. Alexandre, S. Cabaço, "How do seagrasses grow and spread?," *Eur. seagrasses an Introd. to Monit. Manag.*, in: J. Borum, C.M. Duarte, D. Krause-Jensen,

- T.M Greve (eds.), **European Seagrasses: An Introduction to Monitoring and Management**, The M&MS project, Copenhagen, 2004, pp. 11-18.
- [82] J. Jiménez-Casero, M.D. Belando, J. Bernardeau-Esteller, L. Marin-Guirao, R. Garcia-Munoz, J.L. Sanchez-Lizaso, J.M. Ruiz, *A Critical Gap in Seagrass Protection: Impact of Anthropogenic Off-Shore Nutrient Discharges on Deep Posidonia oceanica Meadows*, **Plants**, **12**(3), 2023, Article Number: 457. DOI: 10.3390/plants12030457.
-

Received: July 7, 2024

Accepted: April 25, 2025